Available online at www.sciencedirect.com
SCIENCE DIRECT®
Composites: Part A 34 (2003) 719–730
composites
Part A: applied science and manufacturing
www.elsevier.com/locate/compositesa

Transient hygrothermal stresses in fiber reinforced composites: a heterogeneous characterization approach

Pavankiran Vaddadi, Toshio Nakamura*, Raman P. Singh

Department of Mechanical Engineering, State University of New York at Stony Brook, New York, NY 11794, USA

Received 2 October 2002; revised 1 March 2003; accepted 18 March 2003

Abstract

Transient hygrothermal stresses induced in fiber-reinforced composites are studied in detail by adopting a novel heterogeneous characterization approach. This approach incorporates two distinct features: transient moisture absorption analysis of actual composite materials exposed to a humid environment, and highly detailed computational analyses that capture the actual heterogeneous microstructure of the composite. The latter feature is carried out by modeling a uniaxial laminate having more than one thousand individual carbon fibers that are randomly distributed within an epoxy matrix. Results indicate that these computational models are essential in capturing the accurate moisture absorption process of the actual specimen. In the analysis, the evolutions of thermal residual stresses and moisture-induced stresses within the humidity and thermal exposed composites have been analyzed. It was observed that high stress concentration develops in the epoxy phase where high fiber density or fiber clustering exists and its magnitude increases as the moisture content saturates. Large stresses can potentially initiate epoxy damage or delamination of epoxy and fibers. Furthermore, due to opposing effects of thermal and moisture exposure, lower stresses are found in the laminate when both are considered simultaneously.

Keywords: A. Carbon fiber; B. Residual/internal stress; B. Stress relaxation; C. Finite element analysis (FEA); Random fiber model

1. Introduction

Fiber reinforced epoxy matrix composites are widely used as essential aerospace components and in other structural applications as they offer outstanding mechanical properties and flexibility in design. Despite inherent advantages over conventional structural materials, such as metals, composites are susceptible to heat and moisture when operating in harsh and changing environmental conditions. When exposed to humid environments, carbon–epoxy composites absorb moisture and undergo dilatational expansion. This moisture absorption leads to changes in the thermophysical, mechanical and chemical characteristics of the epoxy matrix by plasticization and hydrolysis [1–3]. These changes in the polymer structure lower both the elastic modulus and the glass transition temperature [1–6]. The net effect of moisture absorption is the deterioration of matrix-dominated properties such as compressive and transverse strength, interlaminar shear strength, fatigue resistance and impact tolerance [1,4,5,7,8]. These factors lead to reduced damage tolerance and lack of long-term durability. In a recent study it was found that moisture absorption can lead to a decrease in transverse modulus of the composite owing to hydrolysis and irreversible plasticizaton of the epoxy matrix [9].

Moisture absorption characteristics of composites have been the subject of considerable investigation [10,11] where transient moisture diffusion under normal environmental conditions is approximated as a Fickian process and analytical models have been developed based on a homogenized model. In homogeneous materials, the transport of moisture is governed by the maximum moisture content, usually a strong function of relative humidity, and effective diffusivity, usually a strong function of temperature. While the effective or average property is appropriate for conditions under *equilibrium* or *steady-state*, its applicability for transient moisture transport is, at best, questionable. More specifically, under transient conditions,

* Corresponding author. Tel.: +1-631-632-8312; fax: +1-631-632-8544.
E-mail address: toshio.nakamura@sunysb.edu (T. Nakamura).

1359-835X/03/$ - see front matter © 2003 Elsevier Ltd. All rights reserved.
doi:10.1016/S1359-835X(03)00135-0

the effective or average property may not accurately describe the time variation of moisture content. An additional concern with the homogenized rule-of-mixtures approach is that it ignores the microstructural heterogeneity and cannot determine stress concentrations developed in fiber reinforced composite. Both these issues were addressed in a recent study by the authors [12] where an inverse analysis technique was used to estimate the moisture diffusion parameters and characterize the moisture absorption in fibrous composites while taking into account the microstructural heterogeneity. This study quantified the differences in transient moisture absorption behaviors between the heterogeneous model and the analytical model with effective properties.

The presence of moisture and the stresses associated with moisture-induced expansion can result in lower damage tolerance, with an adverse effect on long-term structural durability. The amount of moisture absorbed by the epoxy matrix is significantly greater than that by the carbon fibers, which absorb very little or no moisture. This results in a significant mismatch in the moisture induced volumetric expansion between the matrix and the fibers, and thus leads to the evolution of localized stress and strain fields in the composite [13]. In addition to the stresses induced due to mismatch in moisture expansion coefficients, stresses are also induced in composites due to a mismatch in coefficients of thermal expansion. The thermal stresses produced while cooling the composites after fabrication at elevated temperature are called thermal residual stresses or curing stresses. These stresses develop due to curing related shrinkage of the matrix and during cooling down from glass transition temperature, T_g, due to greater coefficient of thermal expansion of the polymer matrix than the fibers, which in turn induces compressive stresses in fiber. Hahn and Kim [14] developed analytical results that took into account the curing stresses in composites and compared these results with the experimental data for the transverse and thickness strains of symmetric and unsymmetric laminates. Collings and Stone [15] performed experiments on carbon fiber reinforced epoxy laminates to measure the residual strains and moisture expansion coefficients and presented equations to predict the thermal and hygrothermal strains. Also, Sih and co-workers [16,17] investigated induced hygrothermal stresses by the theory of coupled heat and moisture. But due to mathematical difficulties encountered in the coupled terms, a closed form solution was available for only one-dimensional problems. Chen et al. [18] analyzed linear problems of coupled heat and moisture combining the finite element method with the Laplace Transform technique.

Because the thermal residual stresses that develop in the matrix during cool down are tensile and compressive in the fibers, moisture absorption and associated swelling can offset the tensile stresses in the epoxy. Thus in order to understand the performance of these composites under actual operational conditions, it is important to study the individual as well as the coupling effects of the moisture induced stresses and the thermal stresses. The present paper addresses these effects by analyzing the transient hygrothermal stresses induced in the fiber reinforced composites using a detailed finite element model that accurately represents the cross section of the actual material. In order to understand the individual and combined effects of moisture transport and hygrothermal stresses, the work is divided into three parts, transient moisture induced stress analysis, thermal stress analysis and combined thermal and moisture induced stress analysis. This approach enables us to clarify how these conditions individually and simultaneously affect the internal stress evolution.

2. Computational models

2.1. Material and specimen descriptions

The composite material chosen to examine the effects of moisture induced and thermal residual stresses was IM7/997 8-ply uniaxial Cytec Fiberite composite having a fiber volume fraction of 58%. The IM7/997 system is currently under development for application to aerospace and rotorcraft structures, and is designed to provide higher damage tolerance than currently qualified materials such as IM7/5271-1. The composite system consists of PAN based, 5 μm diameter, IM7 carbon fibers (Hexcel Composites, Inc.) in a 997 matrix, which is a 177 °C (350 °F) curing, thermoplastic modified, toughened epoxy resin with a proprietary formulation. Moisture absorption experiments were conducted using an environmental chamber (Benchmaster BTRS, Tenney-Lunaire, Inc.) with automated cyclic or constant exposure to temperature and humidity. Three different environmental exposure tests were conducted: Relative humidity, $R_H = 50\%$ and 85% both at $T = 85$ °C, and $R_H = 85\%$ at $T = 40$ °C. The last condition was tested to investigate the effects of temperature [12]. The current work addresses the transient hygrothermal stresses induced by considering the specific case of $T = 85$ °C, and $R_H = 85\%$.

Two specimens were used for each exposure condition to provide repeatability. Also, fresh, as-received specimens were used for each exposure condition, so that any material changes introduced by moisture cycling would not affect the measurements. The specimens were preconditioned first by drying them at 50 °C, until no further change in weight was observed. Then the reference dry weight, W_o for each specimen was recorded during the environmental exposure, the weight gains of the specimens were measured every 24 h using a high resolution analytical balance. This balance has a resolution of 0.1 mg, which corresponds to monitoring a weight change that is about $5 \times 10^{-4}\%$ of the specimen

weight. From the periodic weight measurements, the relative weight gain of composite was computed as

$$w_t = \frac{W(t) - W_o}{W_o}. \quad (1)$$

where $W(t)$ is the total weight at time t and W_o is the reference dry weight of the specimen.

To obtain the moisture diffusion parameters, a special experimental procedure based on an inverse analysis technique, using the weight measurements as the input was utilized to determine the diffusivity and the maximum moisture content for the composite [12]. Since the carbon fibers can absorb a very little moisture, their diffusivity and the maximum moisture content were assumed to be zero, and only the diffusion parameters of epoxy matrix were determined.

This process also utilized highly detailed computational models to account for the actual heterogeneous microstructure of the composite. The detailed description of the procedure is given in Ref. [12]. The values of moisture diffusion parameters estimated from the testing and the inverse analysis are listed in Table 1. These material parameters are used as the inputs in the present finite element analysis. The schematic of a thin composite specimen exposed to moisture environment is depicted in Fig. 1. The nominal dimensions of the specimens were 140 mm × 70 mm × 1.2 mm. As the total area of the front and back surfaces is much greater than the area of the specimen edges (by a factor of 37), moisture transport across the specimen edges was neglected. This reduces the problem to a 2D case in which only moisture absorption transverse to the fiber direction is considered.

2.1.1. Constitutive relation

Internal stresses in composites develop as a result of residual strains developing due to mismatch in thermal expansion of the fiber and epoxy and due to moisture absorption by the epoxy. In order to account for these thermal stresses resulting from the fabrication processes, the difference ΔT between the ambient and the stress-free temperature is introduced into the Hooke's law. The absorption of moisture by carbon–epoxy composites results in the development of stress fields associated with moisture-induced expansion. When we consider both thermal stresses as well as moisture induced stresses acting simultaneously, we can describe the constitutive relationship as a linear superposition of both the stresses. The constitutive relationship can thus be written as

$$\sigma_{ij} = \lambda\varepsilon_{kk}\delta_{ij} + 2\mu\varepsilon_{ij} - (3\lambda + 2\mu)(\beta\Delta C + \alpha\Delta T)\delta_{ij}, \quad (2)$$

where λ and μ are the Lame constants, ΔT is the temperature difference, ΔC is the moisture content, α is the coefficient of thermal expansion, taken to be 45×10^{-6}/°C for the epoxy [19] and 7.2×10^{-6}/°C for the fiber [20]. The input values of other material properties are listed in Table 1. The Young's modulus and Poisson's ratio were taken from the IM7/997 specification data sheets provided by Cytec Fiberite, Inc.

Table 1
Materials properties of IM7 carbon fiber and 997 epoxy

Property	IM7 fiber	997 Epoxy
Young's modulus (transverse)	20 GPa [22]	4.14 GPa [9]
Poisson's ratio	0.33 [22]	0.36 [22]
Coefficient of thermal expansion	7.2×10^{-6}/°C [20]	45×10^{-6}/°C [19]
Coefficient of moisture expansion	0	3.24×10^{-3}/%H_20 [19]
Moisture diffusivity ($T = 85$ °C and $R_H = 85\%$)	0	54.4×10^{-14} m^2/s [12]
Maximum moisture content ($T = 85$ °C and $R_H = 85\%$)	0	1.48% [12]
Density	1780 kg/m^3 [9]	1310 kg/m^3 [9]

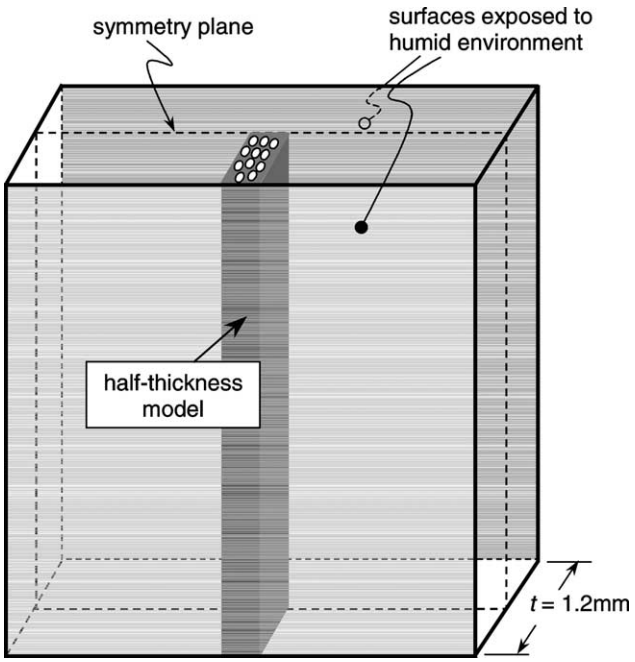

Fig. 1. Thin composite laminate is exposed to humid environment at front and back surfaces. Note the moisture flow from the edges is not considered due to relatively small surface areas. The half-thickness model that is used in the analysis is also illustrated.

2.2. Randomly distributed fiber model

Unlike determination of effective properties of composites under equilibrium and/or steady-state conditions where 'unit cell' models are often used, transient analysis requires the modeling of the *entire length-scale* over which moisture transport occurs. This means one just cannot consider a small region of the specimen to model the transient moisture diffusion behavior. The physical

specimen that was modeled has eight plies accounting for the total thickness of 1.2 mm. Due to the center-plane symmetry, it is necessary to only model half the thickness of the composite. Since the volume fraction and diameter of the carbon fibers are 58% and 5 μm, respectively, and the specimen half-thickness is 600 μm, about one hundred fiber layers can exist from the external surface to the center-plane. Initially, the carbon fibers were arranged in a regularly spaced 'hexagonal arrangement' within the epoxy matrix. This required 111 fibers to generate a model that spans the specimen half-thickness. Such regularly spaced fiber distributions (e.g. hexagonal packing) have been used successfully in many composite analyses for determining effective material properties. However, it has been shown by the authors that they do not capture the moisture transport process of irregularly distributed fibers [12]. Therefore, another model was constructed with many randomly distributed carbon fibers to capture the nature of actual configuration.

In order to model the random fiber arrangements, a computational code was developed to place circular fibers at random positions. Since the specimen has a high fiber volume fraction of 58%, placing every fiber in the domain required special algorithms. Usually no special algorithms are required to generate and place fibers randomly up to 50% volume fraction. Beyond this value computational codes slow down on account of lack of availability of space to place extra fibers, though on a cumulative basis, space is available. Thus an algorithm, which rearranges the current configuration to optimize space availability, is required. In our work, the computational code first generates and places fibers up to a volume fraction of 50% randomly in the specified domain. Then the algorithm for rearranging the fibers is used to optimize the available space. The computational code again starts generating and placing fibers, starting from the updated configuration, calling the rearranging algorithm after every 2% increase in volume fraction. The process is repeated until the desired volume fraction has been generated. Though such fiber placements are not mathematically random, the resulting fiber distribution is clearly irregular and resembles that of actual specimen. Each ply of the specimen was modeled separately and combined together. This allowed for the incorporation of a thin strip of epoxy rich region along ply interfaces, as shown in Fig. 2. In a separate study, it was found that varying the thickness of the epoxy rich region at the ply interfaces had negligible effect on the moisture diffusion process. As discussed earlier, the through thickness dimension of the model must equal the half-thickness of the specimen, i.e. 600 μm, but the width of model is limited by computational resources. A greater width results in the modeling of a larger number of fibers, which requires more computation resources. After several trials, the width of the random model was selected to be 64 μm. This dimension allows for 8–10 fibers to be placed

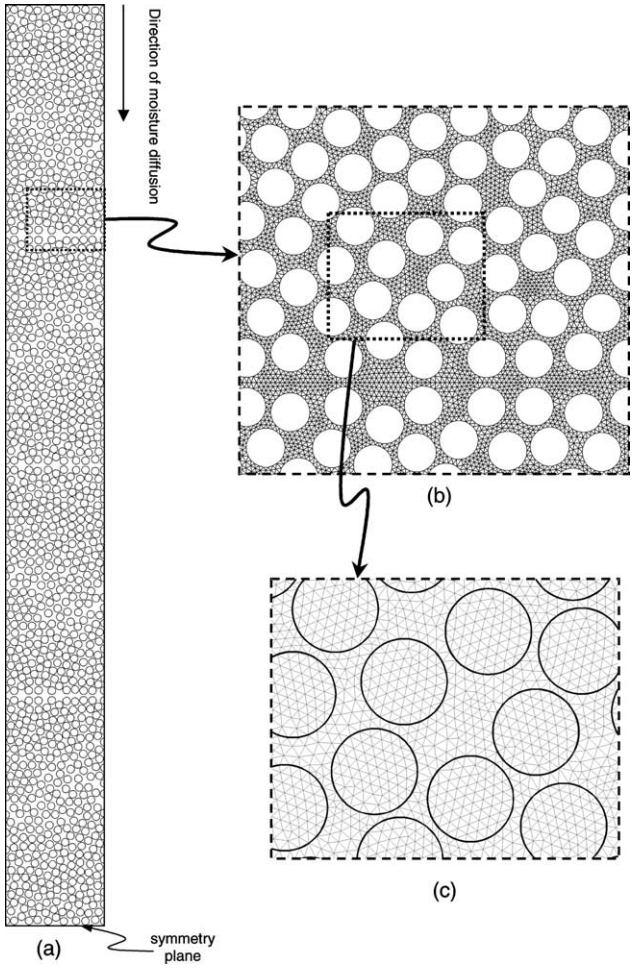

Fig. 2. Schematics of random model used in the transient analysis. (a) Outlines of 1200 fibers are shown in the half-thickness model. (b) Finite element mesh of local region. The elements representing fibers are not shown for clarity. (c) Enlarged view of mesh with fibers.

across the model width without resulting in prohibitively expensive computations.

A total of 1200 fibers were placed in the random fiber model to generate the required fiber volume fraction of 58%, as shown in Fig. 2(a). After establishing the fiber distribution, an automatic mesh generator was used to construct a finite element mesh, shown in Fig. 2(b) and (c). The element sizes in this mesh were kept sufficiently small for accurate simulation of transient moisture transport. The entire mesh contains approximately 130,000 nodes and 240,000 triangular elements. Note that the use of this model requires a more than fifty-fold increase in the computational efforts as compared to that of the hexagonal model. Although detailed convergence analysis was not possible due to its complexity, two other random meshes were constructed to check for the consistency in the solutions using the similar computational process. Fig. 3 shows quarter models of the three random models *A*, *B* and *C*. The results of finite element analysis using these models are discussed next.

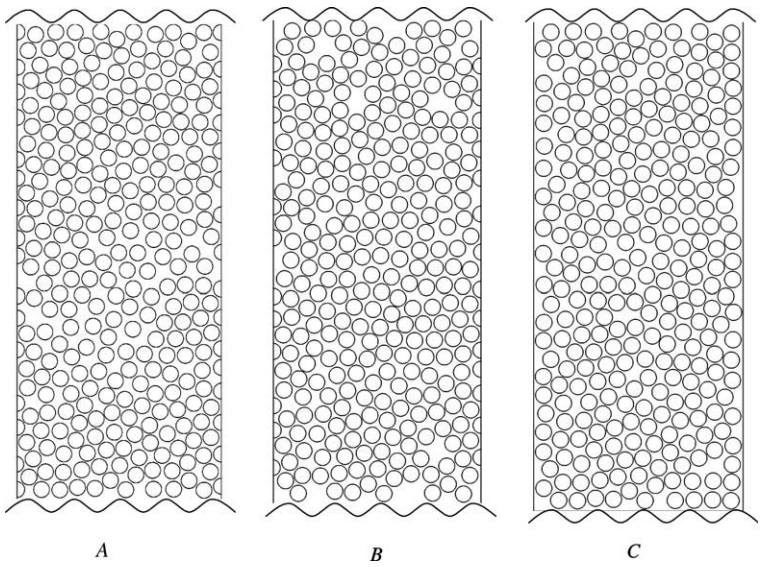

Fig. 3. Schematic of three different random fiber models. Models *A* and *B* contain both full and half-fibers while Model C contains only full fibers. Only a quarter of the model is show for clarity.

2.3. Finite element procedure

Finite element analysis was carried out using the finite element code ABAQUS. Three separate analyses were carried out to study the moisture induced stresses, thermal stresses due to cool-down, and combined hygrothermal stresses. Prior to these stress analyses, the transient moisture transport analysis was carried out to judge the consistency conditions of various models and their accuracy with respect to the experiment. Here three random models and one hexagonal model are used. For each model, the external surface was exposed to the humidity of $R_H = 85\%$ at $t = 0$ and the computation was carried out for 600 h at time increment of 6 h. At each increment, a post-processing code was employed to compute the total moisture content of the entire model through integration over all elements. In order to compare with the experimental measurements, the moisture content was converted to the relative weight gain of the composite. The experimental measurements of relative weight gain, shown in Fig. 4, and series of finite element solutions with the random fiber model, were used in an inverse analysis technique to extract the diffusivity and maximum moisture content of epoxy, and they were estimated as 54.4×10^{-14} m^2/s and 1.48%, respectively, [12]. Note if the hexagonal model were used instead, the estimated diffusivity would have been 45.2×10^{-14} m^2/s (16% lower than that of the random model). The value of diffusivity estimated from the random fiber model would closely, if not exactly, represent the diffusivity of the actual specimen, as any typical cross section of a fiber reinforced composite would have fibers distributed randomly in the epoxy matrix.

The computed time variations of the relative weight gain as well as that of actual composite are shown in Fig. 4. The experimental measurement is an average value obtained from two separate specimens, having the same configuration and dimensions. The difference in the two measurements was minimal with the maximum difference being 0.7% of the weight gain (in terms of the total weight of the specimen, they are $<0.05\%$ apart). This corresponds to about 0.002% along the vertical axis of the Fig. 4. The oscillatory behavior observed for the measured data is due to the fluctuation of condition within the environmental chamber and should not be mistaken as measurement error. A few important observations can be made based on this plot. First, the differences among the three random models $A-C$ are very small. This attests that our random models contain sufficient number of fibers and any variability arising from the models is limited. Second, there is about 7% difference at $t \approx 200$ h between the results of random and hexagonal models.

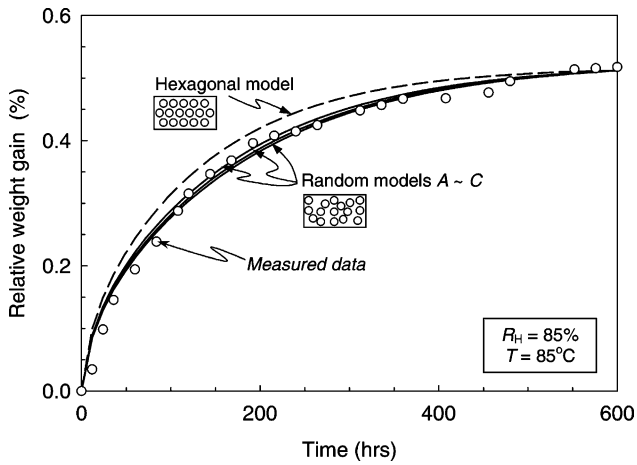

Fig. 4. Time variations of relative weight gain of composites exposed to RH = 85% at $T = 85$ °C condition. The results from three separate random models as well as hexagonal model are shown. The experimentally measured weight gain is also shown with circles.

Though it would appear to be insignificant compared to the fluctuation of measured data, the use of the hexagonal model would have caused 16% lower diffusivity as described in Section 2.2. This is an important factor in using the random model. The discrepancy in the two models is attributed to the different effective moisture flow rates. Fiber clustering generates more resistance to moisture absorption process in the random model, while the moisture transport is easier with uniformly spaced hexagonal model. Third, the agreements between the measured and simulated values of random models are striking. The simulated results remain within the bounds of experimental error throughout the measured time period ($0 < t < 600$ h). The close match between the measured and the simulated values supports the random fiber model to be accurate for the moisture transport analysis. At very long time ($t > 600$ h), all results converged to the same values as the epoxy phase was fully saturated and held the same amount of moisture.

Using the random model *A*, various transient hygrothermal analyses were performed to study the internal stress evolution. In all cases, generalized plane strain elements were employed to allow for out-of-plane deformation. For the boundary conditions, symmetry conditions in moisture, displacements and temperature were imposed along the sides of model except along the exposed surface. For the displacement condition, the three sides were kept straight and the four corners were set to remain perpendicular. The transient moisture induced stress analysis was performed as a coupled temperature displacement analysis. The analogy between Fick's law for mass diffusion and Fourier's law for heat transfer was employed to model transient moisture diffusion [21]. The values of conductivity, specific heat and density, for a heat transfer analysis, were adjusted appropriately to provide the solution for transient moisture diffusion. For the finite element model, moisture transport into the material occurs only across the top surface exposed to the humidity. Thus, it was possible to specify the maximum moisture content for given environmental conditions as the boundary condition on this surface. At time $t = 0$, the entire specimen had zero moisture content. For each case, the computational analysis of moisture diffusion was conducted for more than 600 h in over 100 increments.

The thermal stress analysis due to cool-down was performed as a steady-state heat transfer analysis and constant temperature throughout the specimen was assumed. In the calculation, the temperature drop was directly assigned at every node. No transient thermal stress analysis was conducted since the steady-state condition is reached within seconds as opposed to several hundred hours for the moisture absorption. Note that the thermal conductivity of the composites is of orders higher than its moisture diffusivities. Furthermore, no viscoelastic effects were included although the epoxy is expected to exhibit rate-dependent deformation near the glass-transition temperature. Inclusion of viscoelasticity would not only require additional material parameters but would also require the exact cooling procedure to be specified. This information was not available. However, any stress relaxation due to the rate effects can be approximated with a smaller temperature drop. Several finite element simulations were performed

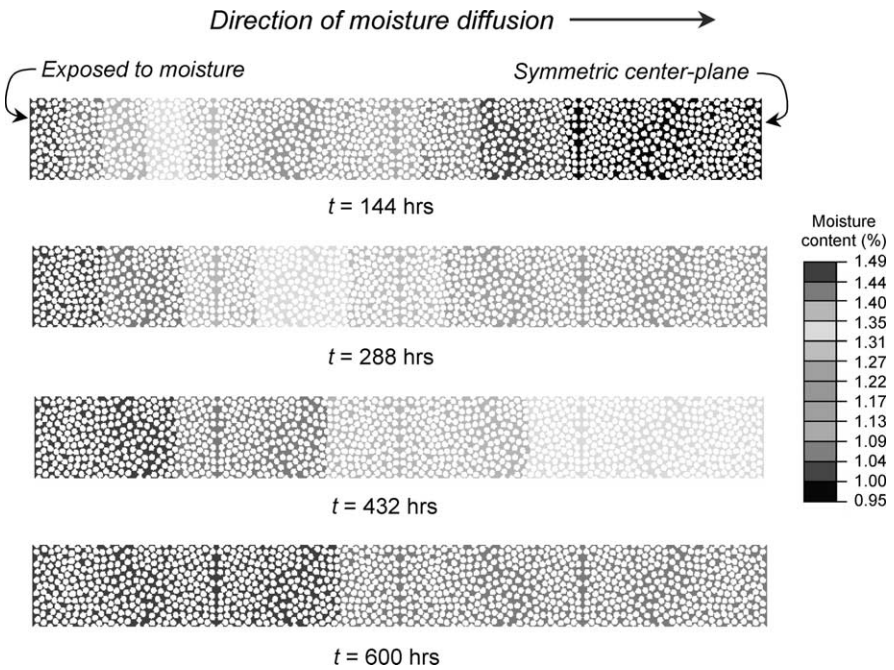

Fig. 5. Shades of transient moisture distribution within epoxy are shown at four different times under $R_H = 85\%$ condition. The moisture permeates from the exposed surface on the left to the center-plane of specimen on the right.

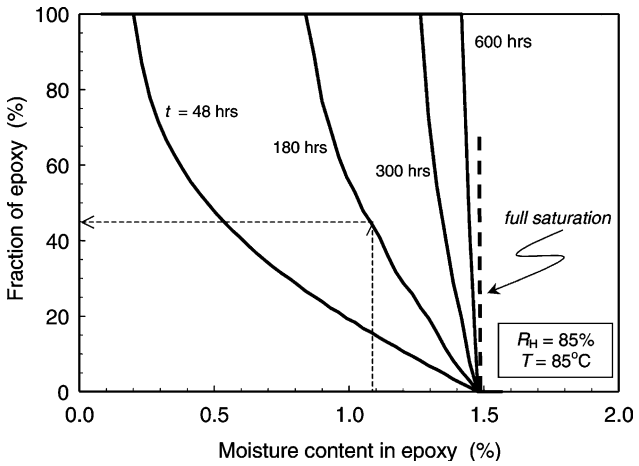

Fig. 6. Fraction of total epoxy phase at or above a given value of humidity level is shown at four different exposure times. As time progresses, the entire model approaches the full saturation at 1.48%.

for various values of temperature drop to see the nature of induced stresses as a function of temperature change. In the combined thermal stress and moisture induced stress analysis, the dilatational expansion/contraction due to thermal as well as moisture loading was considered. Here the analysis was performed in two stages: a steady-state thermal analysis for cool-down, followed by a transient analysis where moisture induced stresses were generated.

3. Transient hygrothermal analysis

3.1. Moisture induced stresses

In the first analysis, the evolutions of transient moisture diffusion and the induced stresses were studied. Fig. 5 illustrates the moisture distribution profiles within the composite as a function of time. The surface is exposed to a humidity of $R_H = 85\%$. The moisture contents of the epoxy phase are shown for four different exposure durations of 144, 288, 432 and 600 h. At region near the moisture-exposed surface, the moisture content immediately saturated and reached the maximum moisture content of $C^* = 1.48\%$. In fact this was the boundary condition prescribed along the exposed plane. Subsequently, the moisture transported towards the symmetric center-plane as time progressed. This process is illustrated by changing color of the epoxy phase from left to right in Fig. 5. At $t = 600$ h, almost the entire epoxy was fully saturated except very near the center-plane. Thereafter, the composite would only absorb a limited amount of moisture and hence only a small additional weight gain would be possible. In order to clarify the evolution of moisture absorption within the composite, fractions of epoxy containing greater than certain humidity levels are plotted in Fig. 6. Here, at a given elapsed time, a percentage of epoxy phase which contains more than a specific value of moisture can be

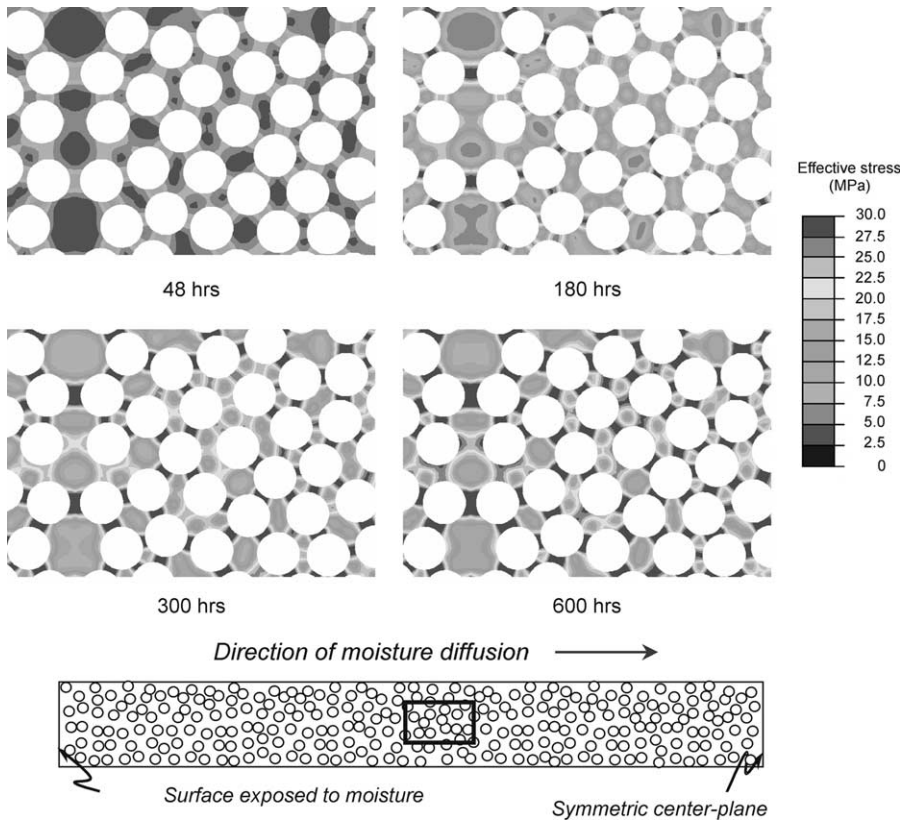

Fig. 7. Varying effective stresses under transient moisture diffusion within the region indicated in the schematic. As moisture content increases, larger stresses develop between fibers. Stresses within carbon fibers are not shown for clarity.

determined. For example, to find the volume fraction of epoxy with moisture level of 1.09% or greater at $t = 180$ h, one would draw a vertical line at 1.09% to intersect with the curve as shown in the plot. Then project the intersection point to the vertical axis to obtain 45% of the total epoxy. This means that after 180 h of exposure, 45% of epoxy phase holds more than 1.09% moisture. These plots were created with a post-processing code that integrates volumes of elements which has more than specified humidity level. The curves indicate that epoxy with a particular humidity level increases with time, and slows down as the model approaches saturation. At $t = 600$ h, the curve is nearly vertical at the saturation limit of 1.48%.

During moisture transport, internal stresses are generated due to the moisture expansion mismatch between the fibers and the epoxy. Transient stress distributions are illustrated in Fig. 7. Here the effective stress of small region near the mid-model is shown at four different elapsed times. The stresses within fibers are not shown for clarity. It can be seen that as time elapses, higher stresses develop especially at locations between neighboring fibers. It appears that this stress concentration is greater with smaller separation distances between fibers, although the secondary influences due to other neighboring fibers also exist. In order to ascertain the overall stress evolution, similar plots as shown in Fig. 6 were constructed for the effective and hydrostatic stresses. Fig. 8(a) shows the fraction of epoxy whose effective stress is greater than

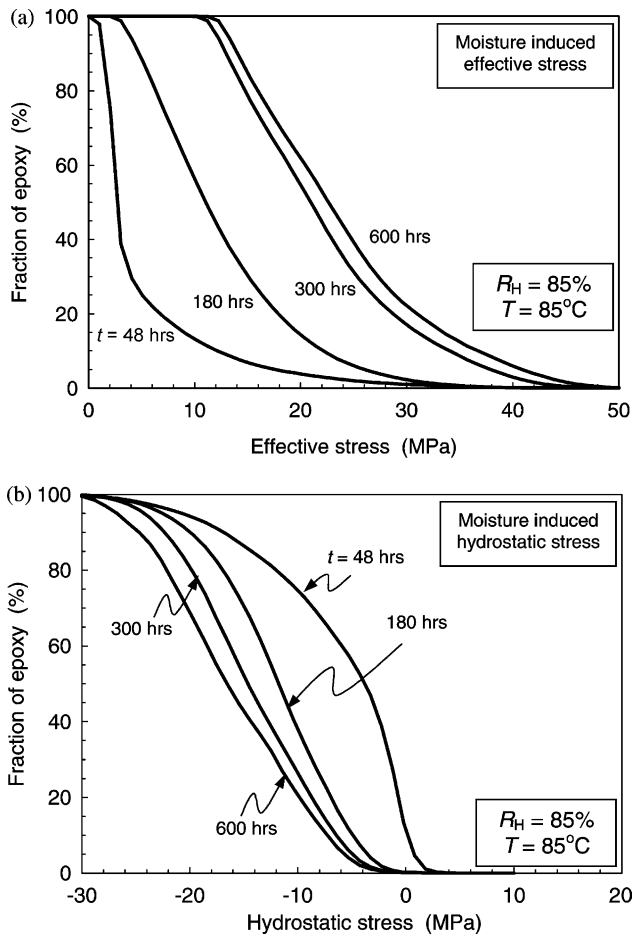

Fig. 8. Fraction of epoxy above a certain value of (a) effective stress and (b) hydrostatic stress at different times during transient moisture absorption.

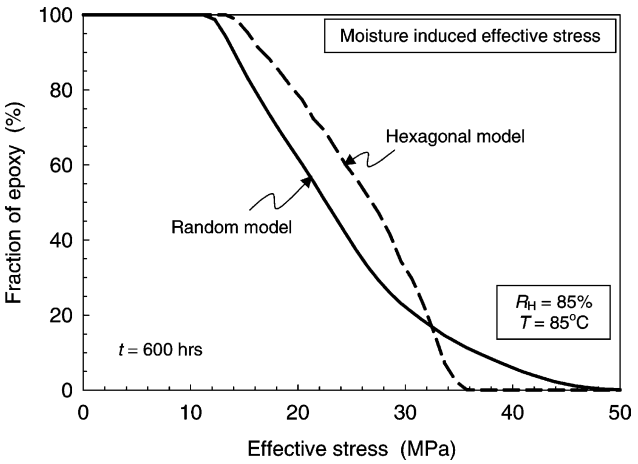

Fig. 9. Fraction of epoxy above a certain effective stress level is shown for the random and hexagonal models, at $t = 600$ h. Note that the hexagonal model reaches a lower stress level compared to the random model.

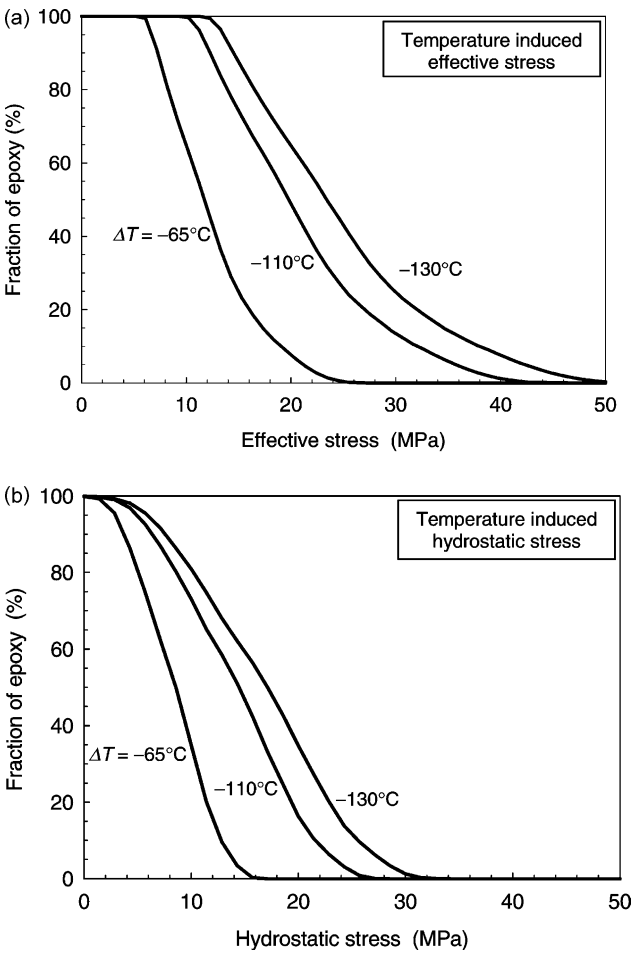

Fig. 10. Fraction of epoxy above a certain value of (a) effective stress and (b) hydrostatic stress is shown for temperature drops of DT = −65, −130 and −150 °C.

certain levels at four different elapsed times. As more moisture seeps through, the moisture-induced stress increases and reaches up to about 50 MPa at $t = 600$ h. Unlike the moisture content shown in Fig. 6, the stress does not reach a uniform state everywhere and a significant spread remains at $t = 600$ h. A similar plot is generated for the hydrostatic stress and shown in Fig. 8(b). A positive hydrostatic stress can lead to delamination of the epoxy from fibers. However, during the moisture absorption, the general state of stress in the epoxy is compression and its magnitude increases with time. During initial phase ($t \approx 48$ h), a small region is in tension.

To make quantitative comparison on stress state between the random and regularly spaced hexagonal fiber distribution models, fractions of epoxy above a certain effective stress level at $t = 600$ h are shown in Fig. 9. The main distinction between the models is the difference in the ranges of stress magnitudes. The range of effective stress in the hexagonal model is about 20 MPa with the peak stress at 34 MPa. However, for the random model, the range is about 36 MPa with the peak level reaching close to 50 MPa. Nearly 50% higher peak stress may lead to significance effects on damage and failure initiation. The random model is more prone to local damages and failure especially in a region where fibers are clustered. Since fibers of actual composites are spaced irregularly, the random model should offer more insight to the actual state of stress than that of the regularly spaced hexagonal fiber model. A similar result was also observed for the hydrostatic stress.

3.2. Thermal stresses

In order to understand the thermal stresses generated during the cool-down, the steady-state thermal analysis was carried out using the random model for three different temperature drops of $\Delta T >= -65, -110$ and -130 °C. These temperatures were chosen since the glass transition temperature of the epoxy is approximately 150 °C and $\Delta T = -65$ °C case corresponds to the ambient temperature of 85 °C in which the moisture absorption experiment was conducted. Also $\Delta T = -130$ °C case represents the temperature decrease to the room temperature. As discussed earlier, no viscoelastic effects were considered and stress relaxation should cause stress magnitudes to be somewhat lowered than those reported here. Unlike the moisture diffusion process, the thermal stress computations were carried out as a time independent process. For each temperature change, the state of field variables was assumed to be in equilibrium.

The results of steady-state thermal analysis are shown for the effective and hydrostatic stress distributions in Fig. 10 for different values of temperature decrease. It is observed

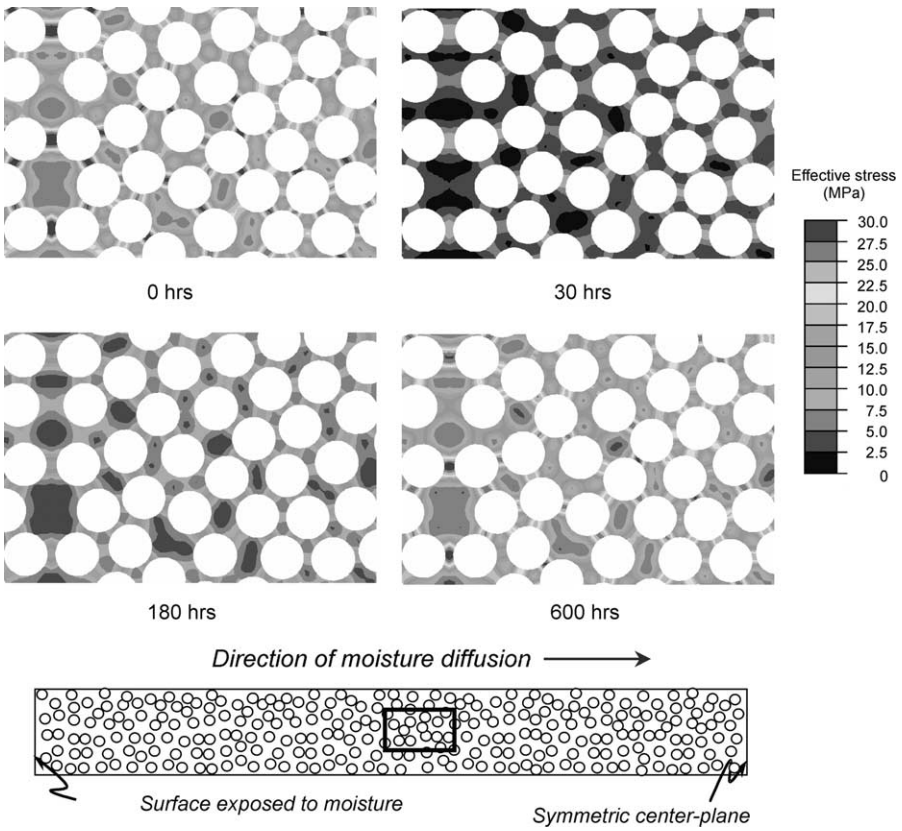

Fig. 11. Varying effective stresses under combined thermal and transient moisture diffusion within the region indicated in the schematic. At $t = 0$, the residual stress due to the temperature drop of DT $= -65$ °C is shown. At the beginning of moisture diffusion, the initially tensile stress relaxes due to the swelling effect of moisture absorption.

that as the magnitude of the temperature change increases the peak effective stress value increases. For the effective stress shown in Fig. 10(a), it increases with greater temperature drop and its peak reaches close to 50 MPa at $\Delta T = -130$ °C. Interestingly, the stress distribution at this temperature drop is very similar to that of the moisture induced stress at $t = 600$ h shown in Fig. 9. But note that the general state of stress is in tension while it was in compression for the moisture-induced case. In order to better understand the thermal stress effects, hydrostatic stress variation was also analyzed. Fig. 10(b) shows the fraction of epoxy above a certain hydrostatic stress level for different temperature decreases. Similar to the previous observation, as the temperature drop increases, the hydrostatic stress increases. At $\Delta T = -130$ °C, the largest hydrostatic stress reaches 30 MPa which may be sufficient to cause interfacial delamination between fibers and matrix.

3.3. Combined thermal and moisture induced stresses

In order to study the simultaneous effects of thermal and moisture induced stresses, a coupled temperature–moisture analysis was performed using the procedure outlined in Section 2.3. Here the expansions due to moisture absorption as well as that due to temperature gradient were taken into account. To include both the temperature drop and the moisture seepage, linear superposition was employed and the net effect of both the variables was modeled as an equivalent moisture condition. Since the thermal conductivity of the composite is much larger than the moisture diffusivity, transient effects due to the cool-down were not considered and it was assumed to occur at $t = 0$. Since the moisture absorption experiment was carried out at 85 °C, the temperature drop was assumed to be $\Delta T = -65$ °C. Fig. 11 shows the effective stress in the epoxy at a specific location after four different exposure times to the humid environment. At $t = 0$, the existing stress is entirely due to the temperature drop and the epoxy is contraction state. Afterwards, the moisture gradually seeps through and the epoxy tends to expand. This causes an interesting change in the stress state of the epoxy. As the time progresses, the effective stress actually decreases due to the offsetting moisture-induced expansion. In fact between $t = 30$ and 180 h, the magnitudes of effective stresses remain very low everywhere. Once more moisture seeps through at a later time, expansion takes over and larger stresses prevail. However, even at $t = 600$ h, peak effective stress is much lower than that for the moisture-only case shown in Fig. 7.

Evolutions of stresses can be better quantified with the plots of the fraction of epoxy above certain stress levels shown in Fig. 12(a). Here, the curve at $t = 0$ is identical to that for $\Delta T = -65$ °C case shown in Fig. 10(a). It represents the residual stress due to the cool-down. As the moisture transports through the composite, this curve initially shifts to the left. This is an indication of stress relaxation due to the canceling of contraction by temperature drop and expansion

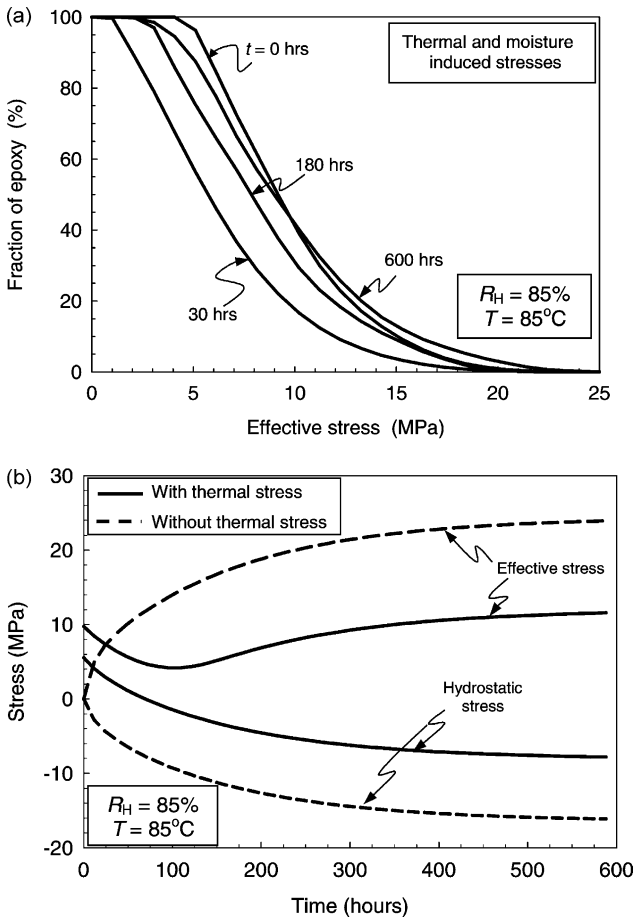

Fig. 12. (a) Fraction of epoxy above a certain value of effective stress at different times. (b) Time variation of average effective stress and hydrostatic stress for models with and without the residual thermal stresses (DT = −65 °C).

by moisture absorption. At later time, the expansion takes over and the curve shifts back to the right. In fact, the curve at $t = 600$ h is similar to that at $t = 0$. Note the peak effective stress level is much lower, about 20 MPa, which is significantly less than that in case of moisture induced stress without thermal stress, shown in Fig. 8(a).

More detailed time evolution of stresses can also be observed in Fig. 12(b). This plot shows the averaged effective and hydrostatic stresses in the entire specimen. The results are shown for the cases with and without the thermal stresses. With the thermal stress case, the average effective stress in the specimen is about 10 MPa at $t = 0$. The average drops to 4 MPa at around $t = 100$ h as moisture is transported to expand the epoxy. Then the average gradually increases as more moisture is absorbed. For one without the thermal stress, the average effective stress continues rise with time. More straightforward results can be observed for the hydrostatic stresses. The decreasing trends of average hydrostatic stress for both with and without the thermal stress are very similar, except that the case with thermal stress is always shifted up by 6–8 MPa throughout the duration of the moisture flow. The average

hydrostatic stress with thermal stress changes from tensile to compressive state at around $t = 70$ h.

4. Discussions

Evolutions of internal stresses within fiber reinforced composites subjected to transient hygrothermal deformation have been analyzed using a novel heterogeneous modeling approach. A simulation study was carried out to follow the actual moisture absorption experiment conducted in the environmental chamber. The detailed finite element model constructed contained well over 1000 individual fibers, and they were distributed randomly so that it captured the important geometrical feature of actual composites. From the comparison study with the regularly fiber distributed model (i.e. hexagonal model) and the experimentally obtained relative weight gain data, we found that modeling of many randomly distributed fibers was critical for obtaining accurate representation of the moisture absorption process.

A methodical approach has been adopted to understand both the individual and combined effects of moisture transport and thermal stresses. This approach enables us to clearly understand how these conditions individually and simultaneously affect the internal stress evolution. First, the internal stress evolution due to transient moisture flow was investigated without a consideration to residual thermal stresses. It was found that the stresses gradually increase from the exposed surface to the interior, as the moisture tends to expand the epoxy phase. The magnitudes of stresses can reach significant level for the random fiber model and these regions would be susceptible to damage initiation, especially where fibers are clustered. Furthermore, it was found that the regularly spaced hexagonal model reached a much lower stress level when compared to the random fiber model, indicating that fiber spacing and arrangement has a significant effect on the induced stresses. In the next analysis, the effects of residual stress due to the cool-down were studied for different values of temperature drops. Unlike the moisture absorption, the contraction caused the epoxy to be in tension.

Subsequently, a combined thermal and moisture induced stress analysis was performed to understand how the two processes govern the evolution of internal stresses. It was found that the thermally induced stresses were relaxed to a certain extent due to the moisture induced expansion of the epoxy. Then the stresses increased as the moisture absorption was increased further. At a glance, the moisture absorption has a beneficial effect on the composite since it would negate the stresses developed during the fabrication process. However, the moisture can cause epoxy to be a weaker material in terms of modulus and toughness degradation. Furthermore, if some debonding has occurred between the fibers and the matrix during the cool-down, the moisture can generate sufficient interfacial shear stress to initiate cracking in the epoxy phase. These behaviors should be highly dependent on local fiber distributions within the composite. It is expected that probability of failure is greater under the randomly distributed fiber condition than with a regularly arranged fiber case.

Acknowledgements

We gratefully acknowledge the US Army Research Office and the National Science Foundation for supporting this research under grant numbers DAAD19-00-1-0518 and CMS 0219250, respectively. We are also thankful to Mr J. Morris and Mr S. Fattohi of Cytec-Fiberite Inc., Anaheim, CA for donating the IM7/997 composite laminates used in this project.

References

[1] Weitsman YJ. Fatigue of composite materials. New York: Elsevier; 1991.
[2] Jones FR. Reinforced plastics durability. Cambridge: Woodhead Publishing Company; 1999.
[3] Zheng Q, Morgan RJ. Synergistic thermal-moisture damage mechanisms of epoxies and their carbon–fiber composites. J Compos Mater 1993;27(15):1465–78.
[4] Adams RD, Singh MM. The dynamic properties of fiber-reinforced polymers exposed to hot, wet conditions. Compos Sci Technol 1996; 56(8):977–97.
[5] Zhao SX, Gaedke M. Moisture effects on mode II delamination behavior of carbon/epoxy composites. Adv Compos Mater 1996;5(4): 291–307.
[6] Choi HS, Ahn KJ, Nam JD, Chun HJ. Hygroscopic aspects of epoxy/carbon fiber composite laminates in aircraft environments. Compos Part A: Appl Sci Manuf 2001;32(5):709–20.
[7] Soutis C, Turkmen D. Moisture and temperature effects of the compressive failure of CFRP unidirectional laminates. J Compos Mater 1997;31(8):832–49.
[8] Sala G. Composite degradation due to fluid absorption. Compos Part B-Engng 2000;31(5):357–73.
[9] Bhavesh GK, Singh RP, Nakamura T. Degradation of carbon fiber reinforced epoxy composites by ultraviolet radiation and condensation. J Compos Mater 2001;36(24):2713–33.
[10] Shen CH, Springer GS. Moisture absorption and desorption of composite materials. In: Springer GS, editor. Environmental effects on composite materials. Lancaster: Technomic; 1977. p. 2–20.
[11] Browning CE, Husman GE, Whitney JM. Moisture effects in epoxy resin matrix composites. Proceedings of Symposium on Composite Materials: Testing and Design. ASTM STP 617, Philadelphia, PA: American Society for Testing and Materials; 1977. p. 481–96.
[12] Vaddadi P, Nakamura T, Singh RP. Inverse analysis for transient moisture diffusion through fiber reinforced composites. Acta Mater 2003;51(1):177–93.
[13] Lee MC, Peppas NA. Models of moisture transport and moisture-induced stresses in epoxy composites. J Compos Mater 1993;27(12): 1146–71.
[14] Hahn HT, Kim RY. Swelling of composite laminates. Proceedings of Advanced Composite Materials—Environmental Effects. ASTM STP 658, Philadelphia, PA: American Society for Testing and Materials; 1978. p. 98–120.

[15] Collings TA, Stone DEW. Hygrothermal effects in CFRP laminates: strains induced by temperature and moisture. Composites 1985; 307–16.
[16] Sih GC, Shih MT, Chou SC. Transient hygrothermal stresses in composites: coupling of moisture and heat with temperature varying diffusivity. Int J Engng Sci 1980;18:19–42.
[17] Sih GC, Ogawa A. Transient thermal change on a solid surface: coupled diffusion of heat and moisture. J Therm Stress 1982;5: 265–82.
[18] Chen TC, Weng CI, Chang WJ. Transient hygrothermal stresses induced in general problems by theory of coupled heat and moisture. ASME J Appl Mech 1992;59:s10–s16.
[19] Tsotsis TK, Weitsman Y. Energy release rates for cracks caused by moisture absorption in graphite/epoxy composites. J Compos Mater 1990;24:483–96.
[20] Elseifi MA. A new scheme for the optimum design of stiffened composite panels with geometric imperfections. PhD thesis, Aerospace and Ocean Engineering, Virginia Polytechnic Institute and State University; 1998.
[21] Lundgren JE, Gudmundson P. Moisture absorption in glass fiber/epoxy laminates with transverse matrix cracks. Compos Sci Technol 1999;59:1983–91.
[22] Morris J. Private communication. Cytec-Fiberite, Inc., Anaheim, CA; 2001.